

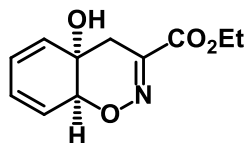
Supporting Information

Identification of inhibitors of CD36-Amyloid beta binding as potential agents for Alzheimer's disease

Deborah Doens^{1,2}, Pedro A. Valiente³, Adelphe M. Mfuh⁴, Anh X. T. Vo⁴, Adilia Tristan¹, Lizmar Carreño¹, Mario Quijada¹, Vu T. Nguyen⁴, George Perry^{4,5}, Oleg V. Larionov⁴, Ricardo Leonart¹, Patricia L. Fernández^{1*}

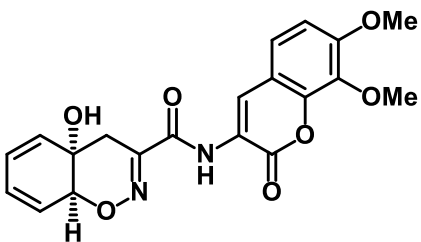
Experimental Procedures

(4a*S,8a*S**)-Ethyl 4a-hydroxy-4a,8a-dihydro-4*H*-benzo[*e*][1,2]oxazine-3-carboxylate ¹ (7)**



(4a*S,7*R**,8a*S**)-Ethyl 7-((methoxycarbonyl)oxy)-4a-hydroxy-4a,7,8,8a-tetrahydro-4*H*-benzo[*e*][1,2]oxazine-3-carboxylate ¹ (2.0 g, 6.4 mmol)** was dissolved in toluene (32 mL), and the solution was degassed by bubbling argon for ~15 min. Freshly distilled *N,O*-bis(trimethylsilyl)acetamide (BTSA) (1.4 mL, 7.0 mmol) was added, and the mixture was continuously degassed for an additional 20 min. Tetrakis(triphenylphosphine)palladium (0.74 g 0.64 mmol) was added, and the mixture was stirred for 10 min. The mixture was directly loaded onto a silica gel column (12 g silica gel) and eluted with a 70:30 v/v mixture of hexanes and 5 vol % solution of triethylamine in ethyl acetate to give diene **7** as a pale yellow viscous oil (1.3 g, 5.76 mmol, 90%). – ¹H NMR (500 MHz, CDCl₃): 5.96–5.87 (4 H, m), 4.74 (1 H, m), 4.25 (2 H, q, *J* = 10 Hz), 2.75 (1 H, d, *J* = 15 Hz), 2.55 (1 H, br s), 2.45 (1 H, dd, *J* = 15, 5 Hz), 1.28 (3 H, t, *J* = 10 Hz) ppm. – ¹³C NMR (125 MHz, CDCl₃): 163.0, 150.3, 134.4, 129.2, 126.7, 124.7, 80.1, 66.0 62.3, 29.0, 14.2 ppm. – IR: 3349, 3051, 2984, 1714, 1602, 1256 cm⁻¹. – MS (ESI): 246.0 [M+Na⁺].

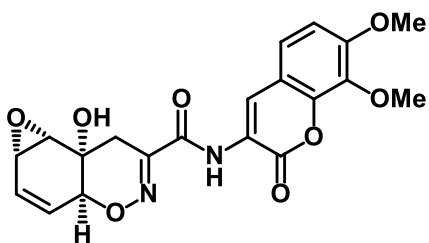
(4a*S,8a*S**)-*N*-(7,8-Dimethoxy-2-oxo-2*H*-chromen-3-yl)-4a-hydroxy-4a,8a-dihydro-4*H*-benzo[*e*][1,2]oxazine-3-carboxamide ¹ (4)**



To a solution of diene **7** (0.3 g, 1.3 mmol) in dichloromethane (7 mL) was added 3 Å molecular sieves (30 mg). The reaction mixture was stirred until the starting material dissolved. Sodium trimethylsilanolate (0.15 g, 1.3 mmol) was added, and the reaction mixture was stirred until

the solution gelled (over 10 min) Methanol (0.2 mL) was added to the gel, and the mixture was swirled until a solution was formed. The mixture was azeotroped with benzene (4×2 mL), and methanesulfonic acid (0.13 g, 1.3 mmol) and dichloromethane (2 mL) were added. The mixture was concentrated under reduced pressure and azeotroped with benzene (2×2 mL). To the resulting solid material was added (1-[bis(dimethylamino)methylene]-1*H*-1,2,3-triazolo[4,5-*b*]pyridinium 3-oxide hexafluorophosphate (HATU) (0.51 g, 1.3 mmol), *sym*-collidine (0.16 g, 1.3 mmol) and 3-amino-7,8-methoxy-2*H*-chromen-2-one (0.3 g, 1.3 mmol). *N,N*-Dimethylformamide (10 mL) was added, and the mixture was stirred at room temperature overnight. Water (20 mL) was added, and the precipitated solid was isolated by filtration through a G4 fritted-glass funnel. The precipitate was washed with water (5×5 mL), and the solid was dissolved in ethyl acetate, dried over anhydrous sodium sulfate, filtered and concentrated under reduced pressure to give an oily material. The desired product was isolated by dissolving the oil in dichloromethane and precipitating amide **4** with hexanes as a colorless solid (0.36 g, 0.91 mmol, 70%). – m.p. 118–123°C. – ¹H NMR (500 MHz, CDCl₃): 9.31 (1 H, s), 8.52 (1 H, s), 7.11 (1 H, d, *J* = 10 Hz), 6.83 (1 H, d, *J* = 10 Hz), 6.00–5.99 (4 H, m), 4.73 (1 H, m), 3.91 (3 H, s), 3.87 (3 H, s), 2.64 (1 H, d, *J* = 10 Hz), 2.55–2.51 (1 H, dd, *J* = 10, 5 Hz) ppm. – ¹³C NMR (125 MHz, CDCl₃): 161.1, 158.2, 154.3, 151.0, 144.4, 136.33, 134.4, 128.7, 127.1, 125.0, 124.6, 122.7, 121.3, 114.3, 109.6, 79.9, 65.9, 61.8, 56.6, 27.6 ppm. – IR: 3356, 2943, 2835, 1714, 1681, 1606, 1521 cm⁻¹. – MS (ESI) 398.0 [M⁺]. – HRMS: calcd. for C₂₀H₁₉N₂O₇⁺ 399.1187, found 399.1175 [M+H⁺].

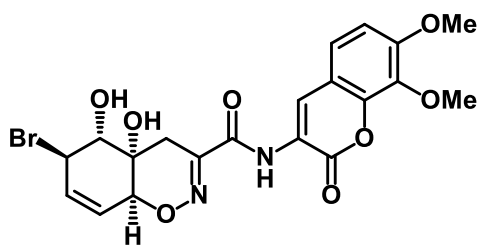
(1a*S*^{*},3a*S*^{*},7a*S*^{*},7b*S*^{*})-*N*-(7,8-Dimethoxy-2-oxo-2*H*-chromen-3-yl)-7a-hydroxy-3a,7,7a,7b-tetrahydro-1a*H*-oxireno[2',3':5,6]benzo[1,2-*e*][1,2]oxazine-6-carboxamide¹ (3**)**



To a solution of amide **7** (0.3 g, 0.7 mmol) in dichloromethane (4 mL) containing sodium bicarbonate (0.1 g, 1.1 mmol) was added a 32 wt % solution of peracetic acid

in acetic acid (0.24 mL, 1.1 mmol) at 0 °C. The mixture was stirred for 1 h, and then concentrated under reduced pressure. The resulting oil was azeotroped with benzene (3 × 10 mL) then dissolved in dichloromethane (1 mL). Addition of hexanes (10 mL) led to precipitation of epoxide **3** (0.29 g, 0.69 mmol, 99%). – m.p. 118–123 °C. – ¹H NMR (500 MHz, **CDCl**₃): 9.41 (1 H, s), 8.59 (1 H, s), 7.19 (1 H, d, *J* = 5 Hz), 6.91 (1 H, d, *J* = 5 Hz), 6.10–6.07 (1 H, ddd, *J* = 10, 4.4, 3.5 Hz), 5.97–5.95 (1 H, ddd, *J* = 10, 4.4, 2 Hz), 4.7 (1 H, m), 3.99 (3 H, s), 3.95 (3 H, s), 3.73 (1 H, d, *J* = 4.4 Hz), 3.52–3.51 (1 H, ddd, *J* = 5.5, 4, 2 Hz), 3.49 (1 H, s), 2.76–2.75 (1 H, dd, *J* = 19.5, 2 Hz), 2.28–2.24 (1 H, d, *J* = 19.5 Hz) ppm. – ¹H NMR (500 MHz, *d*₆-acetone): 9.34 (1 H, s), 8.57 (1 H, s), 7.40 (1 H, d, *J* = 9 Hz), 7.14 (1 H, d, *J* = 9 Hz), 6.15–6.13 (1 H, ddd, *J* = 10, 4.4, 3.5 Hz), 5.92–5.90 (1 h, ddd, *J* = 10, 4.4, 2 Hz), 4.66 (1 H, m), 3.96 (3 H, s), 3.90 (3 H, s), 3.72 (1 H, d, *J* = 4.4 Hz), 3.61 (1 H, m), 3.52 (1 H, s), 2.72–2.68 (1 H, dd, *J* = 19.5, 2 Hz), 2.24–2.20 (1 H, d, *J* = 19.5 Hz) ppm. – ¹³C NMR (125 MHz, **CDCl**₃): 162.7, 159.8, 156.3, 150.7, 146.0, 138.0, 137.2, 128.8, 125.2, 124.6, 123.2, 116.0, 111.8, 78.4, 67.3, 62.4, 60.5, 57.8, 50.7, 26.8 ppm. – IR: 3759, 1712, 1683 1625, 1075 cm⁻¹. – MS (ESI) 414.1 [M⁺]. – HRMS: calcd. for C₂₀H₁₉N₂O₈⁺ 415.1136, found 415.1193 [M+H⁺].

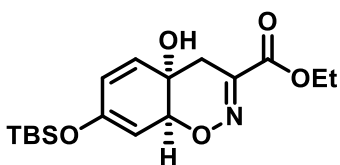
(4a*S*^{*},5*R*^{*},6*R*^{*},8a*S*^{*})-6-bromo-*N*-(7,8-Dimethoxy-2-oxo-2*H*-chromen-3-yl)-4a,5-dihydroxy-4a,5,6,8a-tetrahydro-4*H*-benzo[*e*][1,2]oxazine-3-carboxamide ¹ (6**)**



To a solution of lithium bromide (0.13 g, 0.31 mmol) in THF (3 mL), was added copper dibromide (0.16 g, 0.73 mmol). This mixture was stirred for 10 min, and a solution of epoxide **3** (0.2 g, 0.48 mmol) in THF (4 mL) was added dropwise within 5 min. The reaction mixture was stirred for 1 h. The reaction mixture was poured into a separatory funnel containing saturated aqueous ethylenediaminetetraacetic acid disodium salt (EDTA) solution (15 mL) and ethyl acetate (50 mL). The organic portion was separated and the aqueous phase was extracted with ethyl acetate (2×30 mL). The combined organic fractions were dried over anhydrous sodium sulfate, filtered and concentrated under reduced pressure to give the crude material. Bromohydrin **6** was purified by washing with hexanes. (0.13 g, 0.27 mmol, 86%). – m.p. 120–123 °C. – ¹H NMR (500 MHz, **CDCl**₃): 9.27 (1 H, s), 8.53 (1 H, s), 7.36 (1 H, d, *J* = 9 Hz), 7.07 (1 H, d, *J* = 9 Hz), 6.15–6.12 (1 H, dd, *J* = 10, 2.5 Hz), 5.86–5.83 (1 H, ddd, *J* = 10, 6.5, 2.5 Hz),

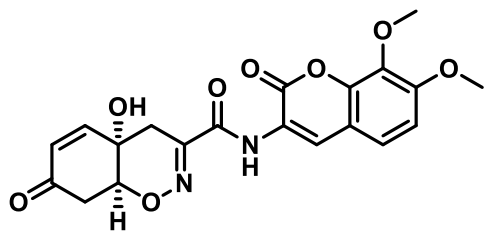
4.8 (1 H, br s), 4.77 (1 H, m), 4.2 (1 H, d, $J = 4.5$ Hz), 3.90 (3 H, s), 3.85 (3 H, s), 3.81 (1 H, d, $J = 5.5$ Hz), 3.42 (1 H, d, $J = 19.5$ Hz), 2.45 (1 H, d, $J = 19.5$ Hz) ppm. – ^{13}C NMR (125 MHz, CDCl_3): 160.5, 157.9, 157.8, 154.4, 151.1, 144.1, 136.1, 135.1, 123.3, 122.9, 114.1, 109.9, 75.6, 73.7, 67.4, 60.5, 55.9, 53.1, 48.9, 22.4 ppm. – IR: 3367, 2928, 2842, 1714, 1677, 1606, 1524 cm^{-1} . – MS (ESI): 495.0 $[\text{M}+\text{H}^+]$. – HRMS: calcd. for $\text{C}_{20}\text{H}_{20}\text{BrN}_2\text{O}_8^+$ 495.0398, found 495.0384 $[\text{M}+\text{H}^+]$.

Ethyl (4a*S,8a*S**)-7-((*tert*-butyldimethylsilyloxy)-4a-hydroxy-4a,8a-dihydro-4*H*-benzo[*e*][1,2]oxazine-3-carboxylate (8)**



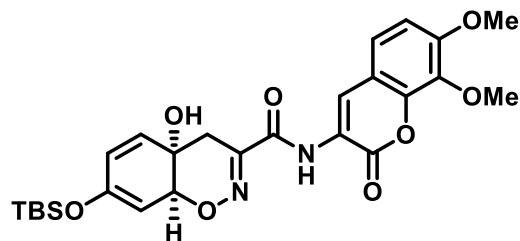
To an oven-dried round bottom flask charged with ethyl (4a*S**,8a*S**)-4a-hydroxy-7-oxo-4a,7,8,8a-tetrahydro-4*H*-benzo[*e*][1,2]oxazine-3-carboxylate (300 mg, 1.24 mmol) and 3 Å molecular sieves (20 mg) in dichloromethane (10 mL) under a gentle flow of argon at 0 °C, was added triethylamine (700mL, 5.02 mmol). Then *tert*-butyldimethylsilyl trifluoromethanesulfonate (600mL, 2.5 mmol) was added dropwise. The mixture was stirred for an hour, and then poured into a separatory funnel containing ethyl acetate (20 mL) and saturated sodium bicarbonate solution (10 mL). The organic phase was separated and the aqueous phase was extracted with ethyl acetate (3×10 mL). The combined organic phases were washed with saturated sodium bicarbonate solution (3×10 mL), dried over anhydrous sodium sulfate, filtered, and the eluent was concentrated under reduced pressure to give the crude product as a waxy solid. This was purified by crystallization from ethyl acetate with hexanes to yield the desired siloxy diene (**8**) as a brown solid (350 mg, 80%). m.p. 101–105 °C. – ^1H NMR (500 MHz, CDCl_3): 5.94 (1 H, d, $J = 10$ Hz), 5.81 (1 H, dd, $J = 10, 2$ Hz), 5.04 (1 H, dd, $J = 5, 2$ Hz), 4.52 (1 H, m), 4.34 (2 H, $J = 7$ Hz), 3.2 (1 H, br s), 2.78 (1 H, d, $J = 19$ Hz), 2.56 (1 H, d, $J = 19$ Hz), 1.37 (3 H, t, $J = 7$ Hz), 0.92 (9 H, s), 0.18 (6 H, s) ppm. – ^{13}C NMR (125 MHz, CDCl_3): 162.9, 151.6, 149.4, 135.4, 128.2, 100.5, 79.1, 64.5, 62.1, 30.3, 25.5, 18.1, 14.1, -4.5 ppm. – IR: 3199, 2930, 2900, 2858, 1716, 1601, 1506, 1464, 1446, 1372, 1251, 1177, 1112, 1017, 910, 836, 781, 709, 623 cm^{-1} . – HRMS: calcd. For $\text{C}_{17}\text{H}_{28}\text{NO}_5\text{Si}^+$ 354.1731, found 354.1728 $[\text{M}+\text{H}^+]$.

(4a*S,8a*S**)-N-(7,8-dimethoxy-2-oxo-2*H*-chromen-3-yl)-4a-hydroxy-7-oxo-4a,7,8,8a-tetrahydro-4*H*-benzo[*e*][1,2]oxazine-3-carboxamide (S1)**



To a solution of (4a*S**,8a*S**)-ethyl 4a-hydroxy-7-oxo-4a,7,8,8a-tetrahydro-4*H*-benzo[*e*][1,2]oxazine-3-carboxylate (1.0 g, 4.2 mmol) in acetone (2 mL) was added phosphate-buffered saline (PBS) (150 mL, 1M, 120 mM, NaCl, pH 7.14) and porcine kidney acylase (200 mg, 1100 U/mg). The mixture was maintained at 25 °C and stirred for 4 days, then lyophilized to a solid material. The solid material was acidified with saturated KHSO₄, and the mixture was extracted with ethyl acetate (4×50 mL). The combined organic portion was dried over anhydrous sodium sulfate, filtered and the eluent was concentrated under reduced pressure to afford a brown solid material. To the resulting solid material was added (1-[bis(dimethylamino)methylene]-1*H*-1,2,3-triazolo[4,5-*b*]pyridinium 3-oxide hexafluorophosphate (HATU) (1.5 g, 4.2 mmol), *sym*-collidine (508 mg, 4.2 mmol), 3-amino-7,8-methoxy-2*H*-chromen-2-one (928 mg, 4.2 mmol) and *N,N*-dimethylformamide (15 mL), and the mixture was stirred at room temperature overnight. Water (20 mL) was added, and the precipitated solid was isolated by filtration through a G4 fritted-glass funnel. The precipitate was washed with water (5×10 mL), and the solid was dissolved in ethyl acetate, dried over anhydrous sodium sulfate, filtered and concentrated under reduced pressure to give an oily material. The desired product **S1** was isolated by dissolving the oil in ethyl acetate and precipitating it with hexane as a brown solid (713 mg, 41%) m.p. 158–162 °C. – ¹H NMR (500 MHz, (CD₃)₂CO): 9.19 (1 H, s), 8.45 (1 H, s), 7.29 (1 H, d, *J* = 8.5 Hz), 7.00 (1 H, d, *J* = 9 Hz), 6.84 (1 H, dd, *J* = 10.5, 1.5 Hz), 5.84 (1 H, d, *J* = 10 Hz), 4.41–4.39 (1 H, m), 3.83 (3 H, s), 3.78 (3 H, s), 2.95–2.91 (1 H, dd, *J* = 17, 3.5 Hz), 2.83–2.79 (1 H, d, *J* = 19 Hz), 2.71–2.68 (1 H, dd, *J* = 19, 1.5 Hz), 2.70 (1 H, br s), 2.60–2.55 (1 H, dd, *J* = 17.5, 7.5 Hz) ppm. – ¹³C NMR (125 MHz, CD₃)₂CO): 194.3, 160.5, 157.9, 154.4, 149.8, 149.3, 144.1, 136.1, 129.6, 123.3, 122.7, 121.3, 114.1, 109.9, 77.6, 62.4, 60.5, 55.9, 38.4, 30.6 ppm. – IR: 3365, 2948, 2844, 1716, 1681, 1627, 1607, 1522, 1108, 995, 842, 660 cm⁻¹. – HRMS: calcd. For C₂₀H₁₉N₂O₈⁺ 415.1136, found 415.1125 [M+H⁺].

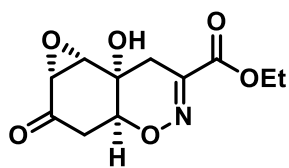
(4a*S,8a*S**)-7-((*tert*-Butyldimethylsilyl)oxy)-N-(7,8-dimethoxy-2-oxo-2*H*-chromen-3-yl)-4a-hydroxy-4a,8a-dihydro-4*H*-benzo[*e*][1,2]oxazine-3-carboxamide (5)**



To a solution of **8** (200 mg, 0.535 mmol), 3Å molecular sieves (20 mg) in dichloromethane (10 mL) under a gentle flow of argon at 0 °C, was added triethylamine (300 mL, 2.122 mmol). Then *tert*-butyldimethylsilyl trifluoromethanesulfonate (245 mL,

1.06 mmol) was added dropwise. The mixture was stirred for an hour, and then poured into a separatory funnel containing ethyl acetate (20 mL) and saturated sodium bicarbonate solution (10 mL). The organic phase was separated and the aqueous phase was extracted with ethyl acetate (3×10 mL). The combined organic phases were washed with saturated sodium bicarbonate solution (3×10 mL), dried over anhydrous sodium sulfate, filtered, and the eluent was concentrated under reduced pressure to give the crude product. This was purified by crystallization from ethyl acetate with hexanes to yield the desired siloxy diene (**5**) as a brown solid (213 mg, 76%) m.p. 104–108 °C. – ¹H NMR (500 MHz, CDCl₃): 9.42 (1 H, s), 8.62 (1 H, s), 7.27 (1 H, d, *J* = 8.5 Hz), 6.92 (1 H, d, *J* = 8.5 Hz), 5.97 (1 H, d, *J* = 10 Hz), 5.86 (1 H, dd, *J* = 10, 2 Hz), 5.08 (1 H, dd, *J* = 5, 2 Hz), 4.54 (1 H, d, *J* = 5 Hz), 4.00 (3 H, s), 3.95 (3 H, s), 2.89 (1 H, d, *J* = 19 Hz), 2.63 (1 H, d, *J* = 19 Hz), 0.95 (9 H, s), 0.22 (6 H, s) ppm. – ¹³C NMR (125 MHz, CDCl₃): 160.9, 158.0, 154.1, 151.7, 150.4, 148.9, 144.1, 136.1, 124.5, 122.7, 120.6, 115.9, 114.1, 109.4, 100.6, 79.4, 64.5, 61.6, 56.3, 28.8, 25.6, 18.0, –4.5 ppm. – IR: 3483, 3363, 2932, 2897, 2855, 1717, 1689, 1605, 1461, 1431, 1374, 1284, 1254, 1229, 1206, 878, 838, 805 cm⁻¹ – HRMS: calcd. for C₂₆H₃₃N₂O₈Si⁺ 529.2001, found 529.2001 [M+H⁺].

Ethyl (1aR*,3aS*,7aS*,7bS*)-7a-hydroxy-2-oxo-1a,3,3a,7,7a,7b-hexahydro-2H-oxireno[2',3':5,6]benzo[1,2-e][1,2]oxazine-6-carboxylate (9)



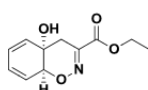
To a solution of ethyl (4aS*,8aS*)-4a-hydroxy-7-oxo-4a,7,8,8a-tetrahydro-4H-benzo[e][1,2]oxazine-3-carboxylate (500 mg, 2.09 mmol) in acetonitrile (11 mL) at 0 °C was added simultaneously DBU (96 mL, 0.63mmol) and 30% hydrogen peroxide (250 mL, 3.14 mmol). The

mixture was stirred for 2 hours, and then extracted with ethyl acetate (30 mL). The ethyl acetate extract was treated with saturated sodium thiosulfate (2×10 mL). The organic portion was dried over anhydrous sodium sulfate, filtered and concentrated under reduced pressure to give the desired material as an oil which crystallized upon standing (373 mg, 70 %). m.p. 66–70 °C. – ¹H

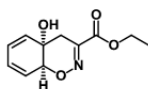
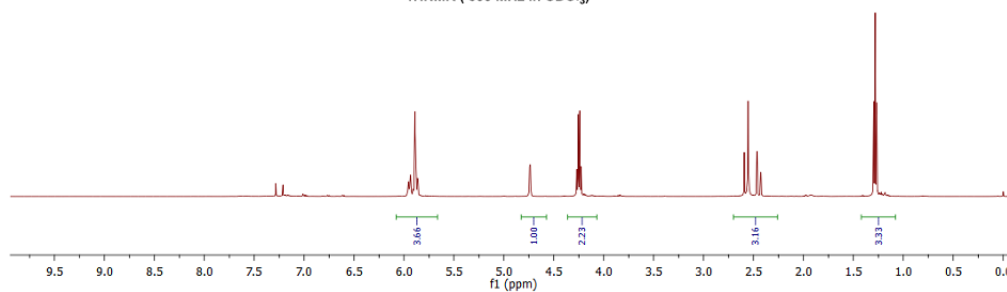
NMR (500 MHz, $\text{CD}_3)_2\text{CO}$): 5.15 (1 H, br s), 4.46–4.43 (1 H, m), 4.29 (2 H, q, $J = 7$ Hz), 3.83 (1 H, d, $J = 3.5$ Hz), 3.40 (1 H, d, $J = 3.5$ Hz), 2.91–2.82 (1 H, dd, $J = 18.5, 5.5$ Hz), 2.83–2.79 (1 H, dd, $J = 19.5, 2$ Hz), 2.74 (1 H, d, $J = 19.5$ Hz), 2.42–2.36 (1 H, dd, $J = 18, 9.5$ Hz), 1.31 (3 H, t, $J = 7$ Hz) ppm. – ^{13}C NMR (125 MHz, $\text{CD}_3)_2\text{CO}$): 200.4, 162.7, 147.4, 73.3, 63.8, 61.4, 60.8, 60.8, 55.8, 38.1, 27.9, 13.5 ppm. – IR: 3318, 2980, 1716, 1601, 1510, 1445, 1372, 1267, 1199, 1092, 974, 974, 856, 831, 747, 711, 649, 585 cm^{-1} . – HRMS: calcd. for $\text{C}_{11}\text{H}_{14}\text{NO}_6^+$ 256.0816.

¹H and ¹³C NMR Spectroscopic Data

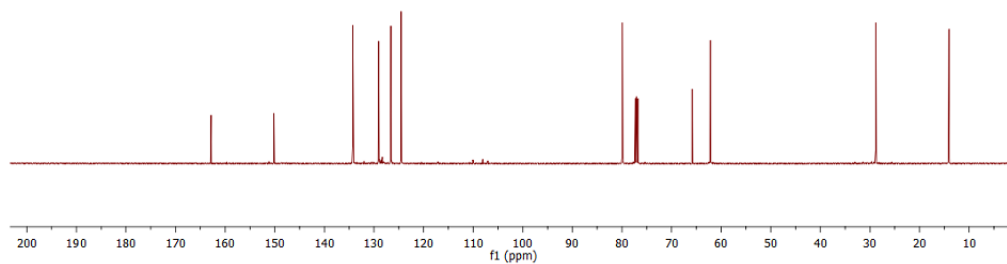
Ethyl (4a*S**,8a*S**)-4a-hydroxy-4a,8a-dihydro-4*H*-benzo[*e*][1,2]oxazine-3-carboxylate (7)



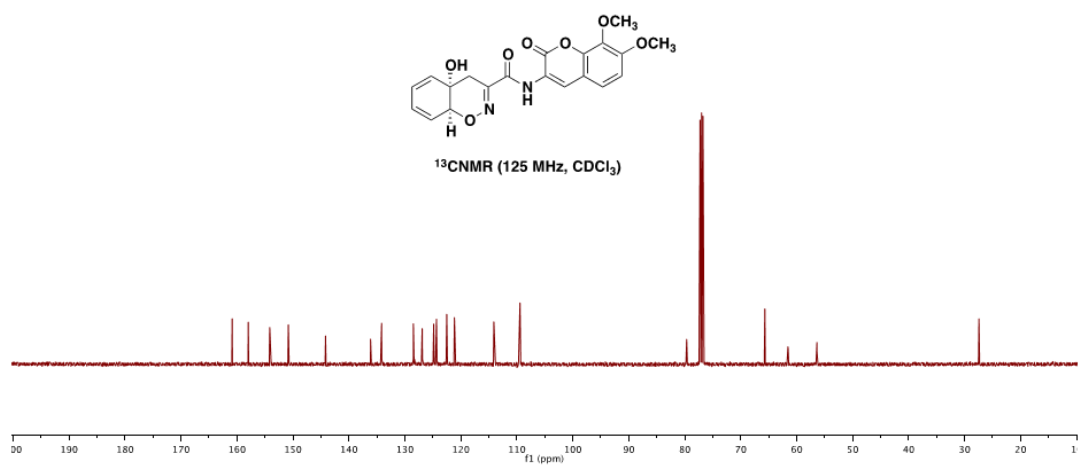
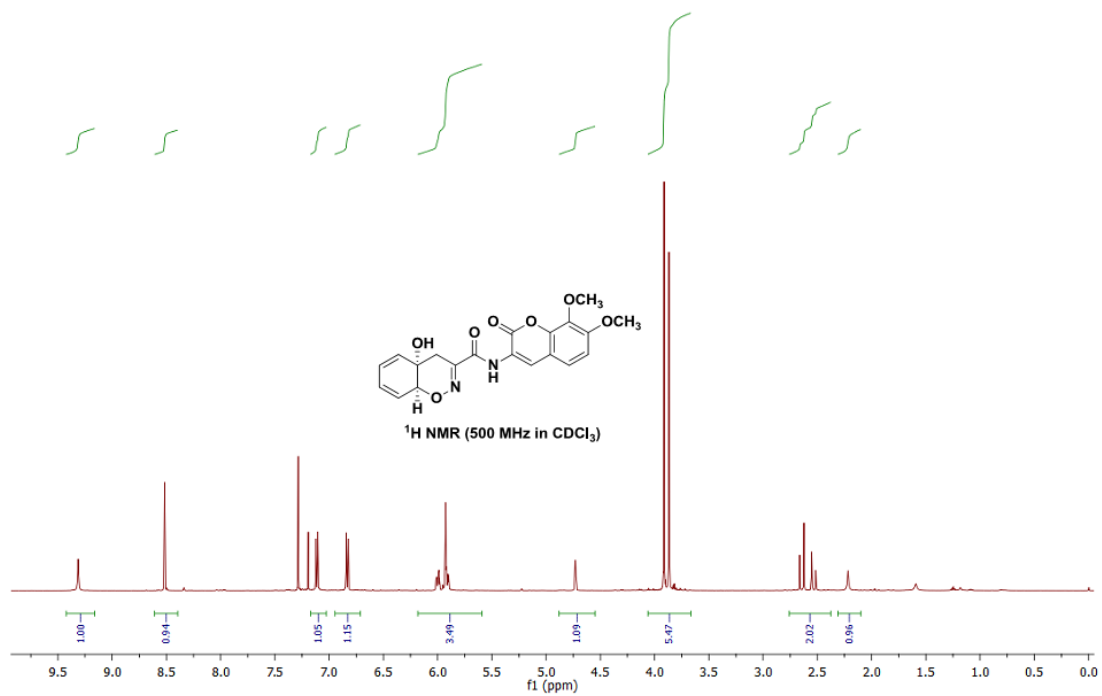
¹H NMR (500 MHz in CDCl₃)



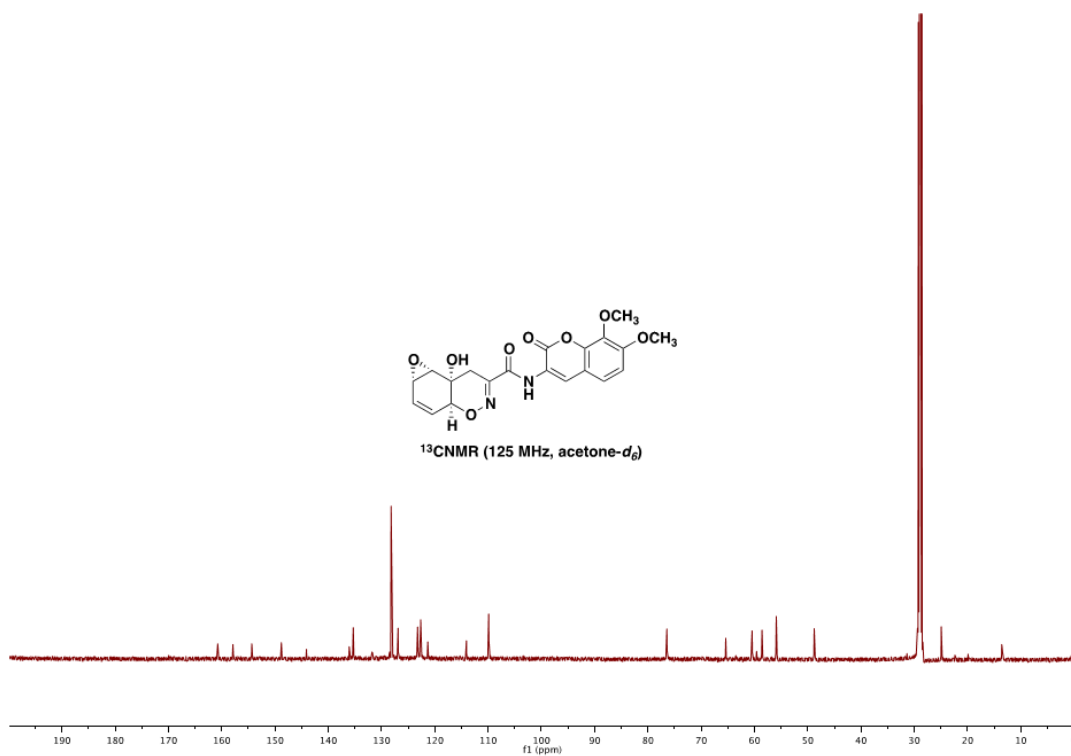
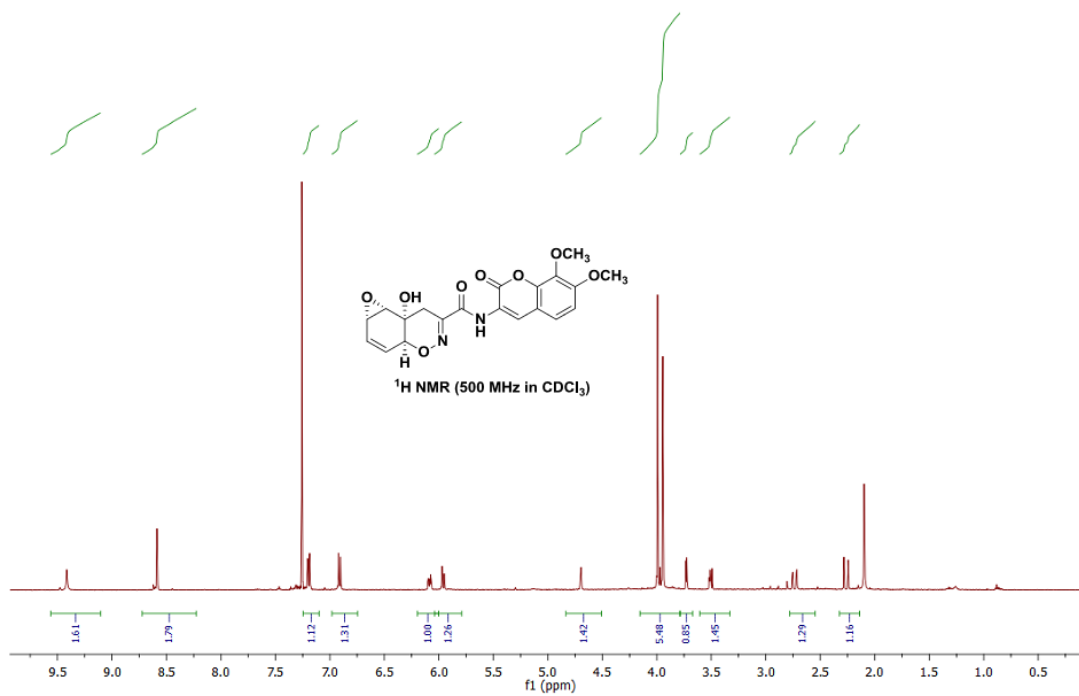
¹³C NMR (500 MHz, CDCl₃)



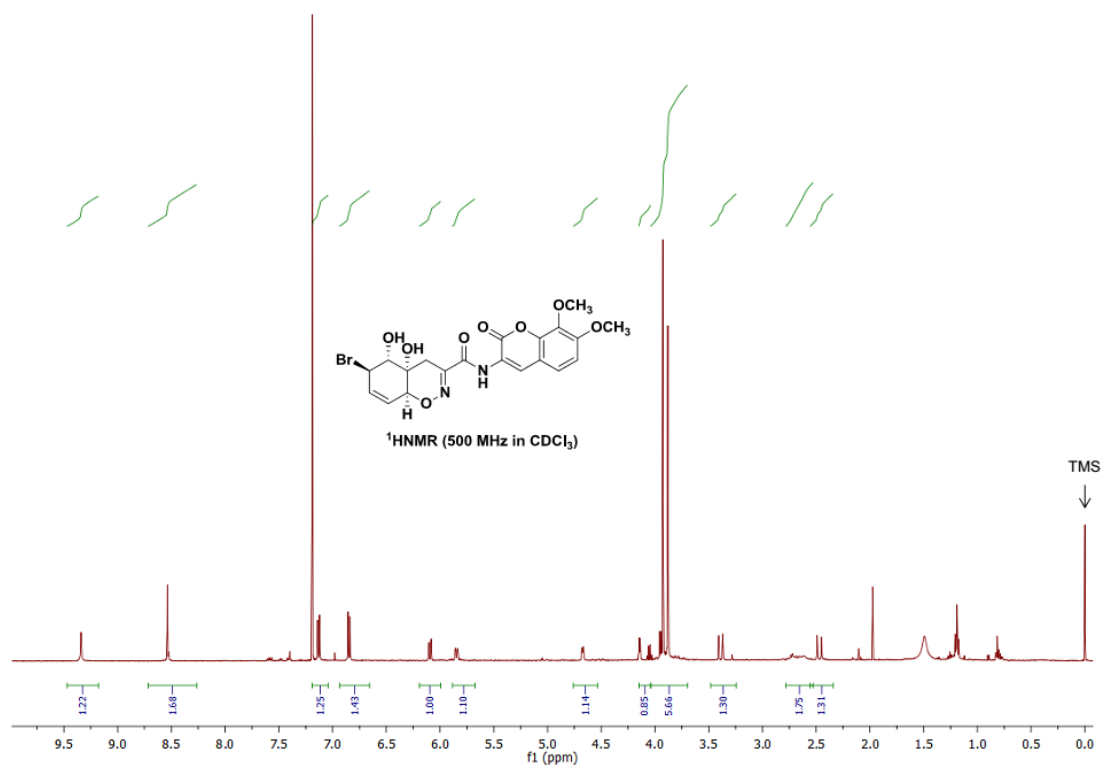
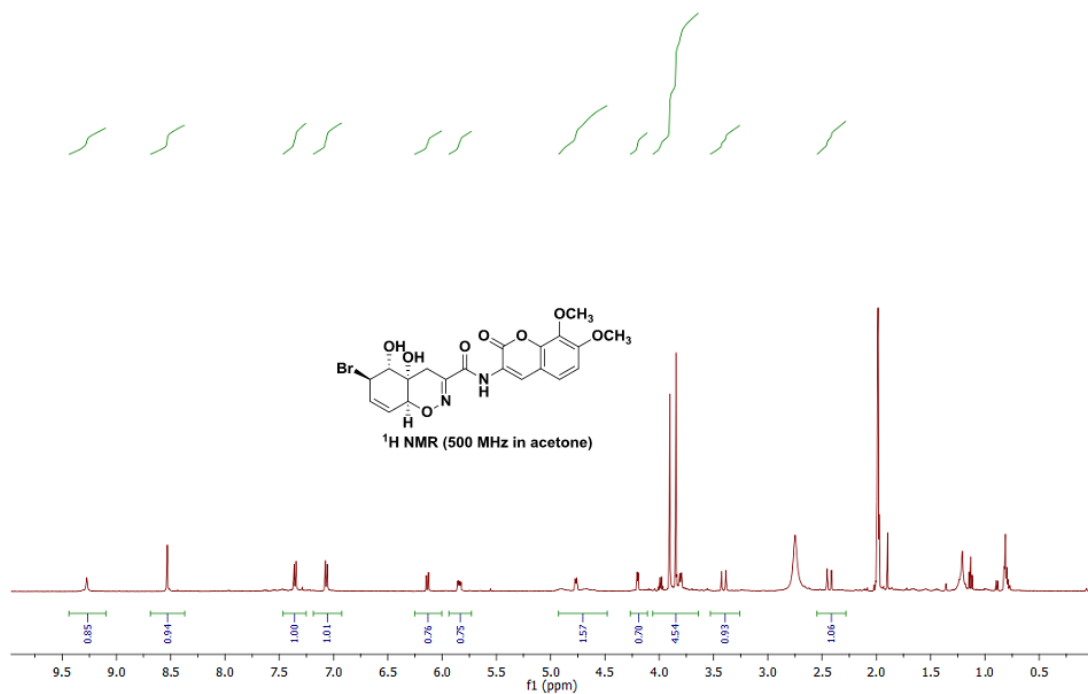
(4aS*,8aS*)-N-(7,8-Dimethoxy-2-oxo-2H-chromen-3-yl)-4a-hydroxy-4a,8a-dihydro-4H-benzo[e][1,2]oxazine-3-carboxamide (4)

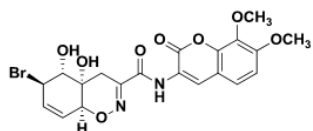


(1a*S,3a*S**,7a*S**,7b*S**)-*N*-(7,8-Dimethoxy-2-oxo-2*H*-chromen-3-yl)-7a-hydroxy-3a,7,7a,7b-tetrahydro-1*H*-oxireno[2',3':5,6]benzo[1,2-*e*][1,2]oxazine-6-carboxamide (3)**

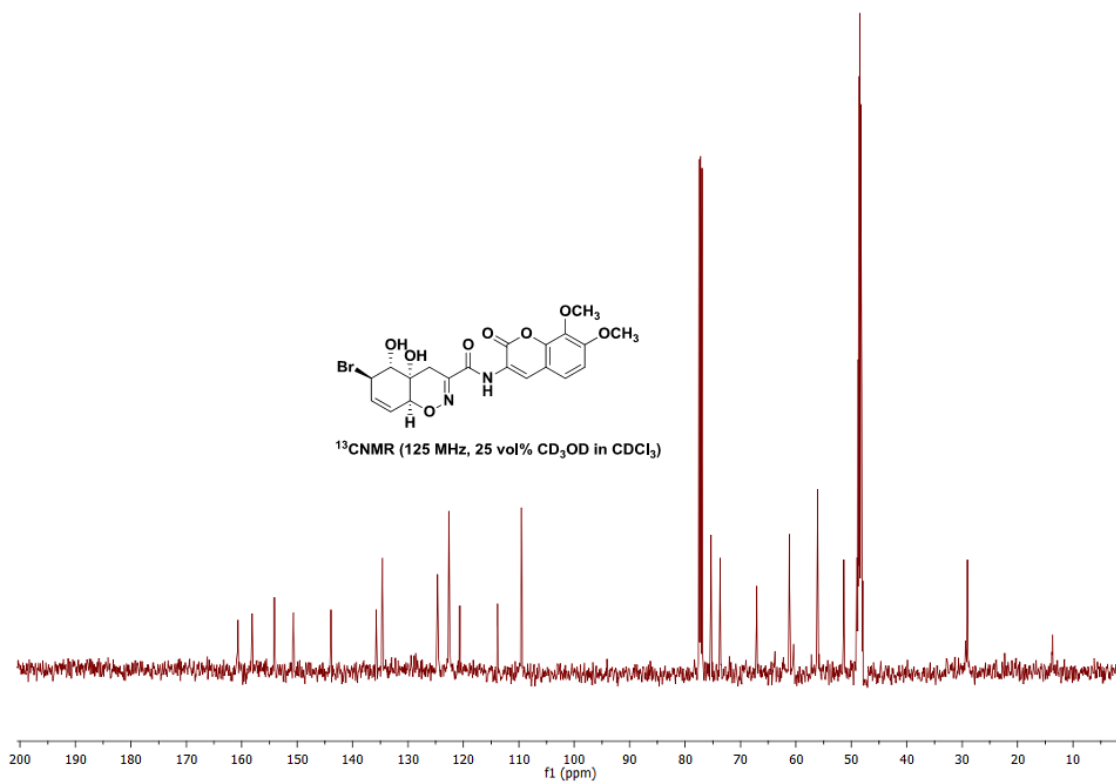


(4a*S,5*R**,6*R**,8a*S**)-6-Bromo-*N*-(7,8-Dimethoxy-2-oxo-2*H*-chromen-3-yl)-4a,5-dihydroxy-4a,5,6,8a-tetrahydro-4*H*-benzo[*e*][1,2]oxazine-3-carboxamide (6)**

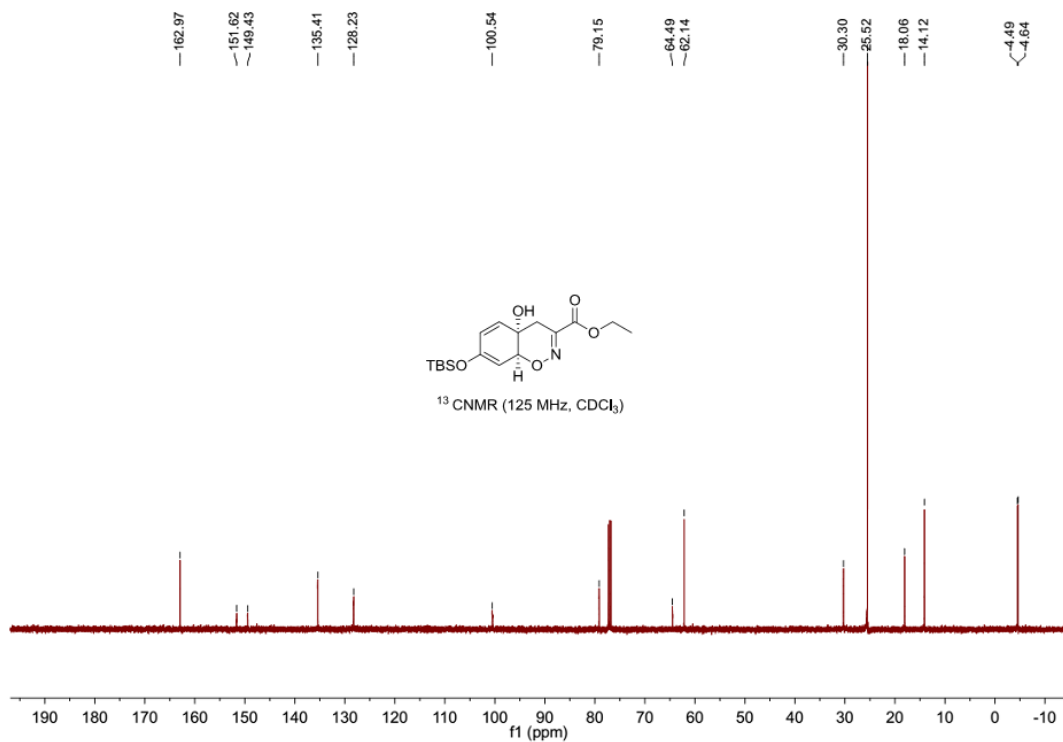
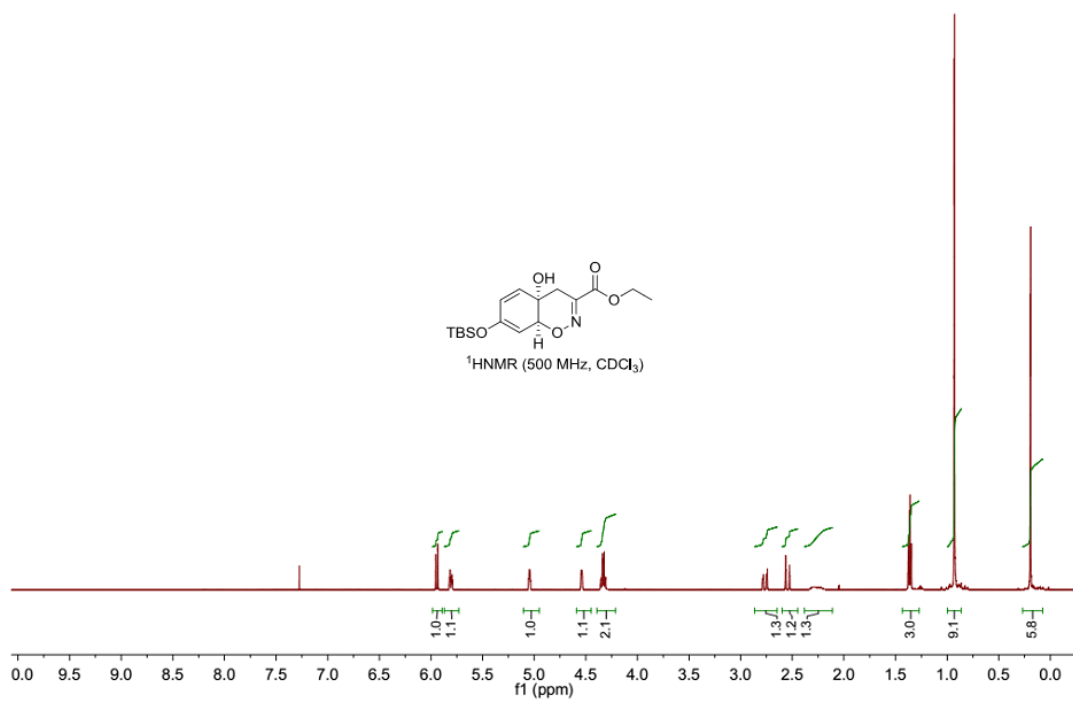




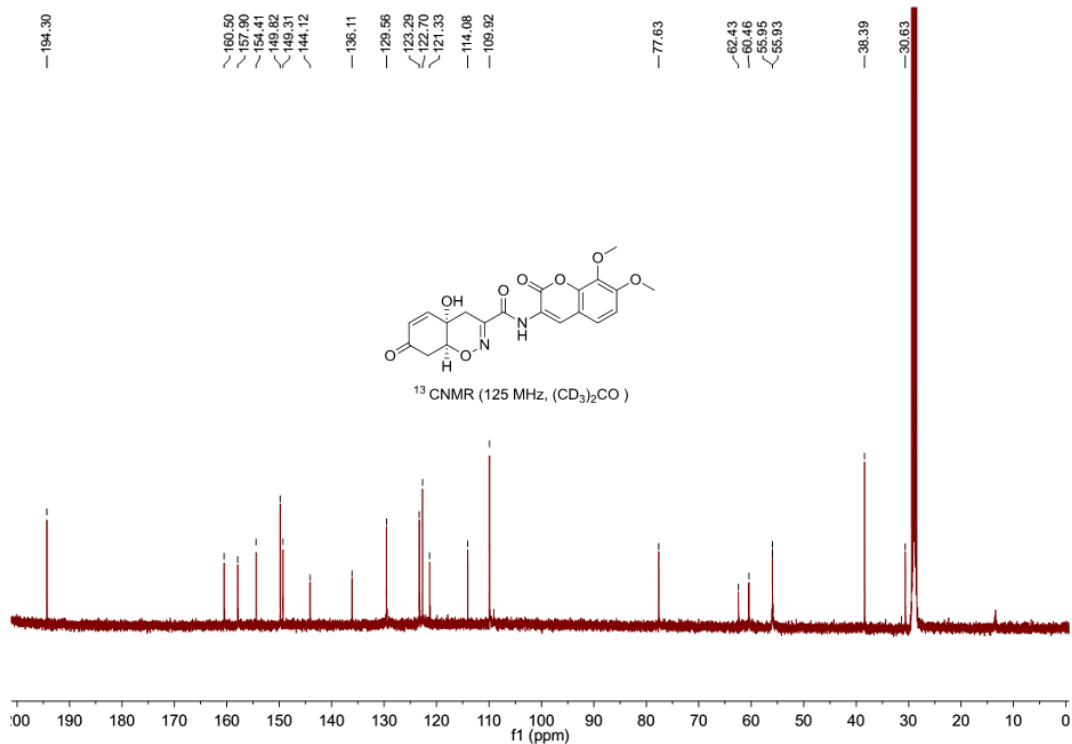
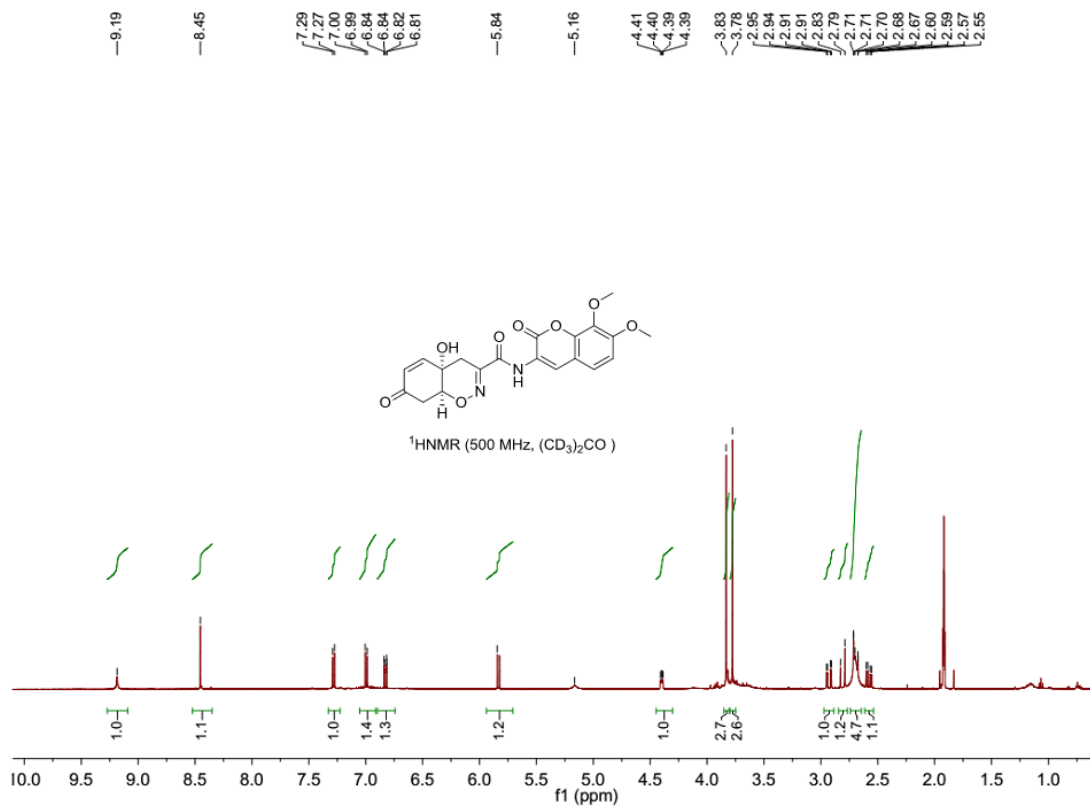
¹³CNMR (125 MHz, 25 vol% CD₃OD in CDCl₃)



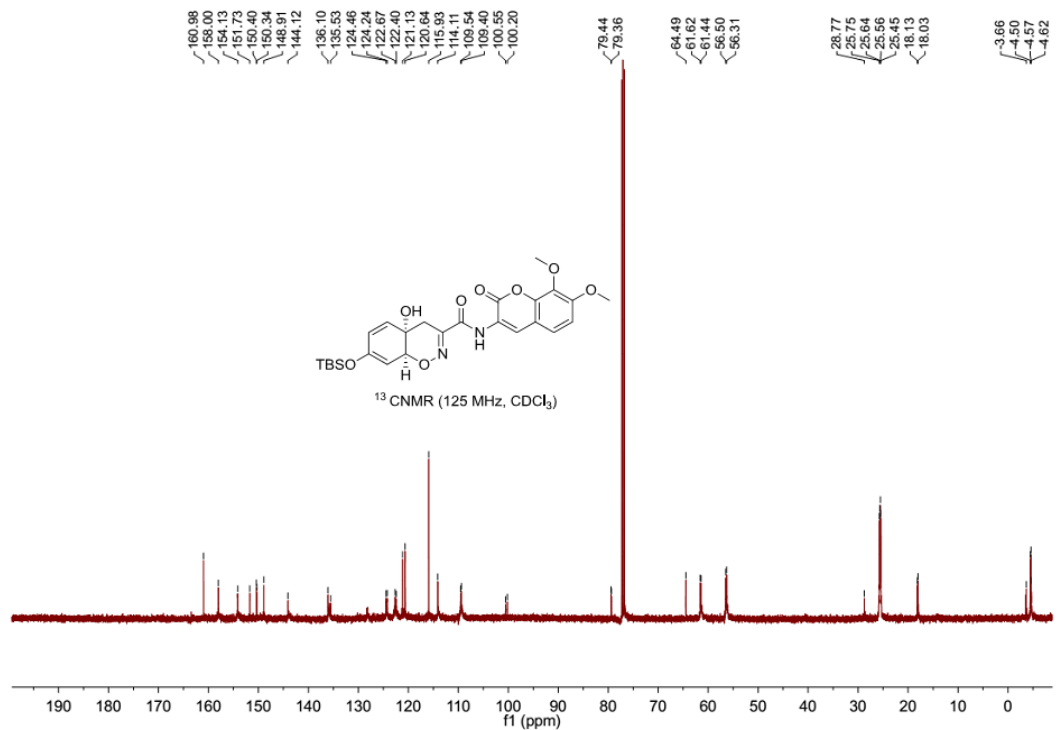
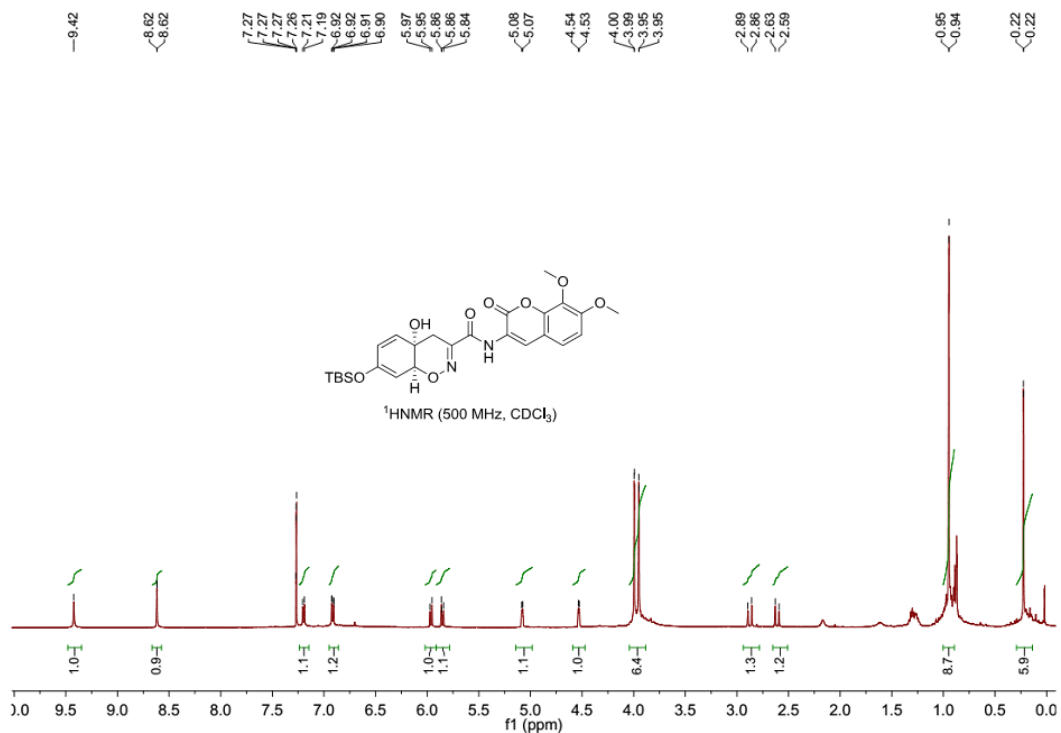
Ethyl (4*aS,8*aS**)-7-((*tert*-butyldimethylsilyl)oxy)-4*a*-hydroxy-4*a*,8*a*-dihydro-4*H*-benzo[*e*][1,2]oxazine-3-carboxylate (8)**



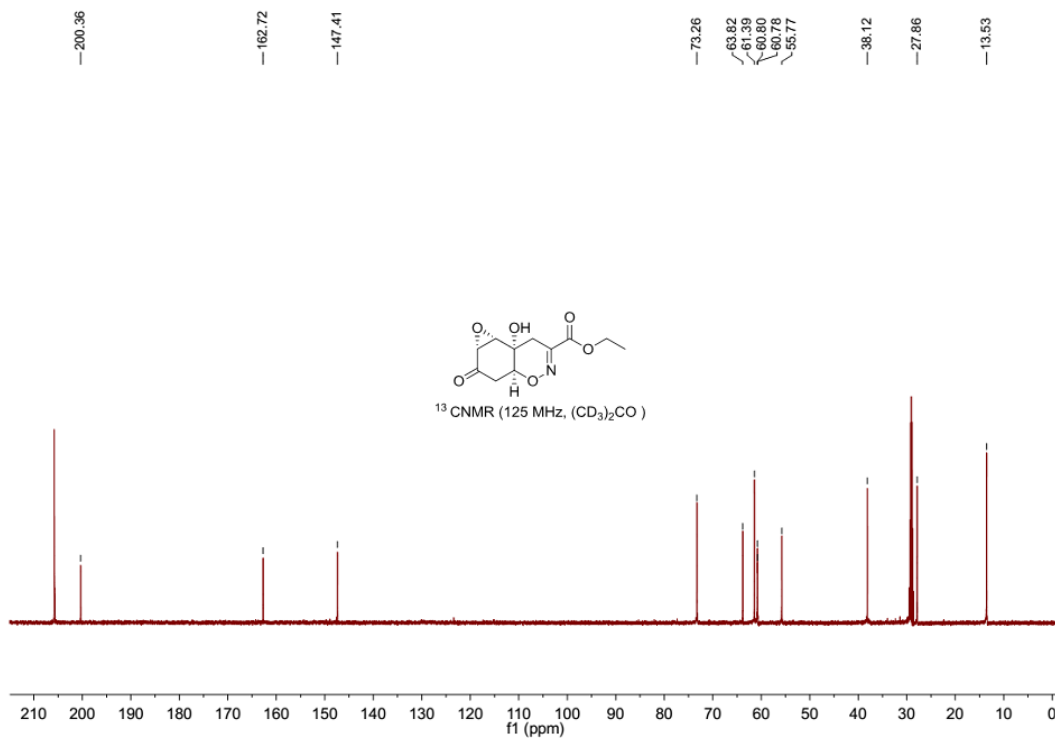
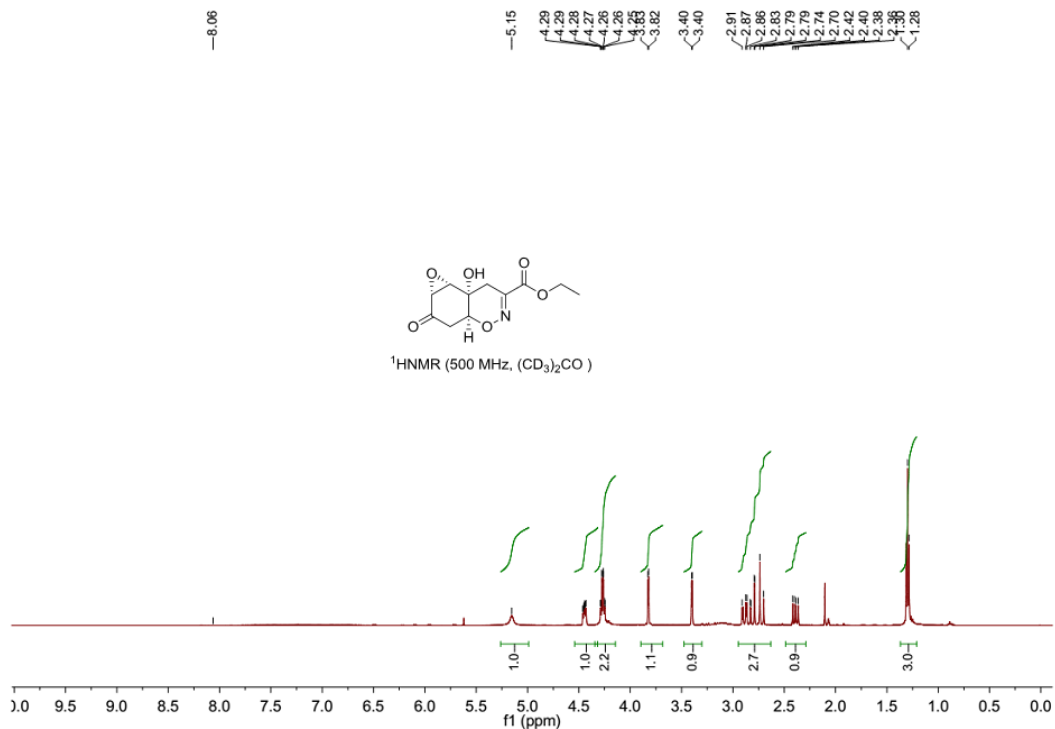
(4a*S,8a*S**)-N-(7,8-Dimethoxy-2-oxo-2*H*-chromen-3-yl)-4a-hydroxy-7-oxo-4a,7,8,8a-tetrahydro-4*H*-benzo[*e*][1,2]oxazine-3-carboxamide (S1)**



(4a*S,8a*S**)-7-((*tert*-Butyldimethylsilyl)oxy)-*N*-(7,8-dimethoxy-2-oxo-2*H*-chromen-3-yl)-4a-hydroxy-4a,8a-dihydro-4*H*-benzo[*e*][1,2]oxazine-3-carboxamide (5)**



Ethyl (1a*R,3a*S**,7a*S**,7b*S**)-7a-hydroxy-2-oxo-1a,3,3a,7,7a,7b-hexahydro-2*H*-oxireno[2',3':5,6]benzo[1,2-*e*][1,2]oxazine-6-carboxylate (9)**



Molecular dynamics simulations procedures. All systems were neutralized (Na^+/Cl^-) and solvated by explicit water molecules, which were modeled by the SPC parameter set², in a cubic box. The distance between the protein-ligand complexes and the edge of the box were set to 10Å. The LINCS algorithm was used to constrain all the covalent bonds in non-water molecules,³ while the SETTLE algorithm was used to constrain bond lengths and angles in water molecules.⁴ Before the production run, systems were relaxed by 1000 steps using a steepest descent algorithm followed by other 1000 steps by conjugate gradient method, where the protein was held fixed by a 10 kcal/molÅ² constraint. Then, systems were gradually heated for 300 ps to reach the experimentally reported assay temperature (for selected systems assay temperature range between 290 and 310K) followed by 200 ps of production run without constraints. The Leapfrog scheme,⁵ with an integration time step of 2 fs was employed to integrate the equations of motion. Temperature was controlled using a weak coupling to a bath with a time constant of 0.1 ps.⁶ For pressure control a Berendsen coupling algorithm with a time constant of 1.0 ps was employed.⁷ Initial velocities were randomly generated from a Maxwell distribution at 1 K, in accordance with the atomic masses.

For production run, Langevin dynamics,⁸ with an integration time step of 2 fs scheme was employed to integrate the motion equations. Temperature was controlled using a weak coupling to a bath with a time constant of 2.0 ps. For pressure control a Parrinello-Rahman⁹ coupling algorithm with a time constant of 5.0 ps was employed. Long range electrostatic interactions were handled by Particle Mesh Ewald (PME) summation.^{10, 11} The van der Waals interactions were modeled by Lennard-Jones (6-12) potential.¹² As in GOMACS is not straightforward to obtain long range electrostatic contributions from PME algorithm, these were recalculated using Reaction Field zero algorithm over the generated trajectory.¹² To ensure that each system was

sufficiently equilibrated before extracting the coordinates for energy calculations, the backbone RMSDs were analyzed. Besides, each simulation was visually inspected to verify its correct behavior.

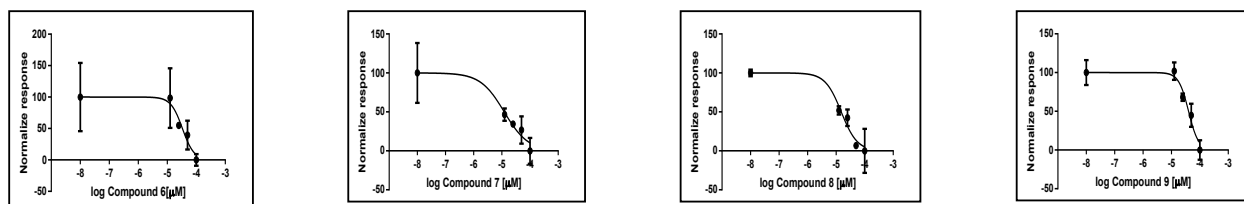
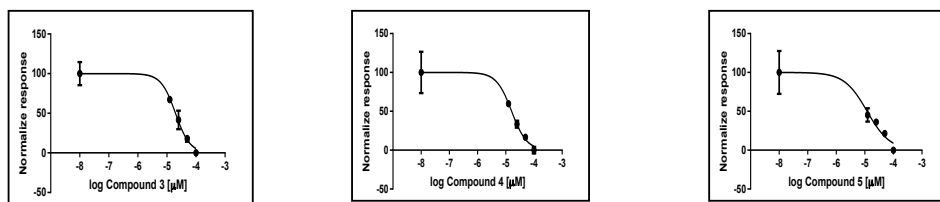


Figure S1: Trichodermamide analogues inhibit the interaction CD36-Aβ. IC₅₀ sigmoidal curves calculated by the statistical software package GraphPad Prism 6 from active compounds shown in Table 1. Graphs represent the sigmoidal curves for the IC₅₀ calculation of a representative experiment. Results represent means ± S.D. from samples assayed in duplicates.

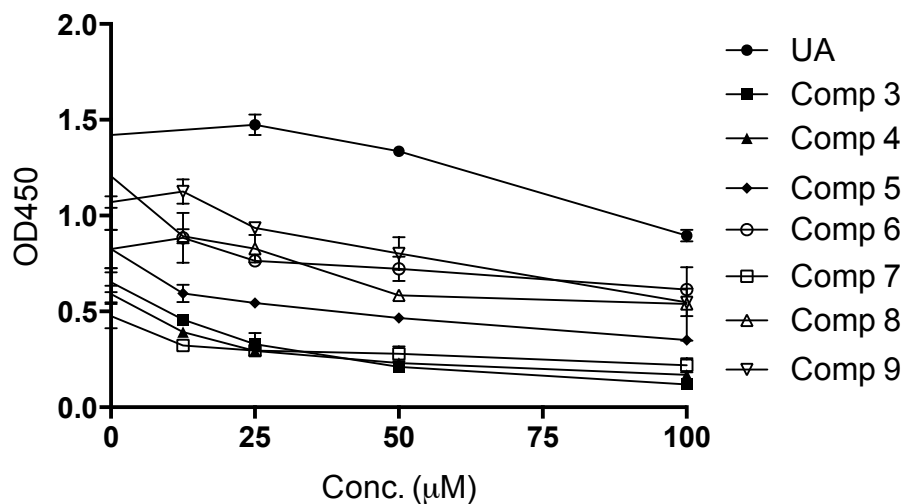


Figure S2: Trichoderamide analogues inhibit in a dose dependent manner the binding of A β to CD36. Trichoderamide analogues were incubated with CD36 in a 96-well plate 30 minutes before the addition of A β . The interaction between CD36 and A β was detected by using an anti-A β primary antibody, a biotin coupled secondary antibody and the HRP enzyme. Results represent means \pm S.E.M. from samples assayed in duplicates and are representative of three different experiments.

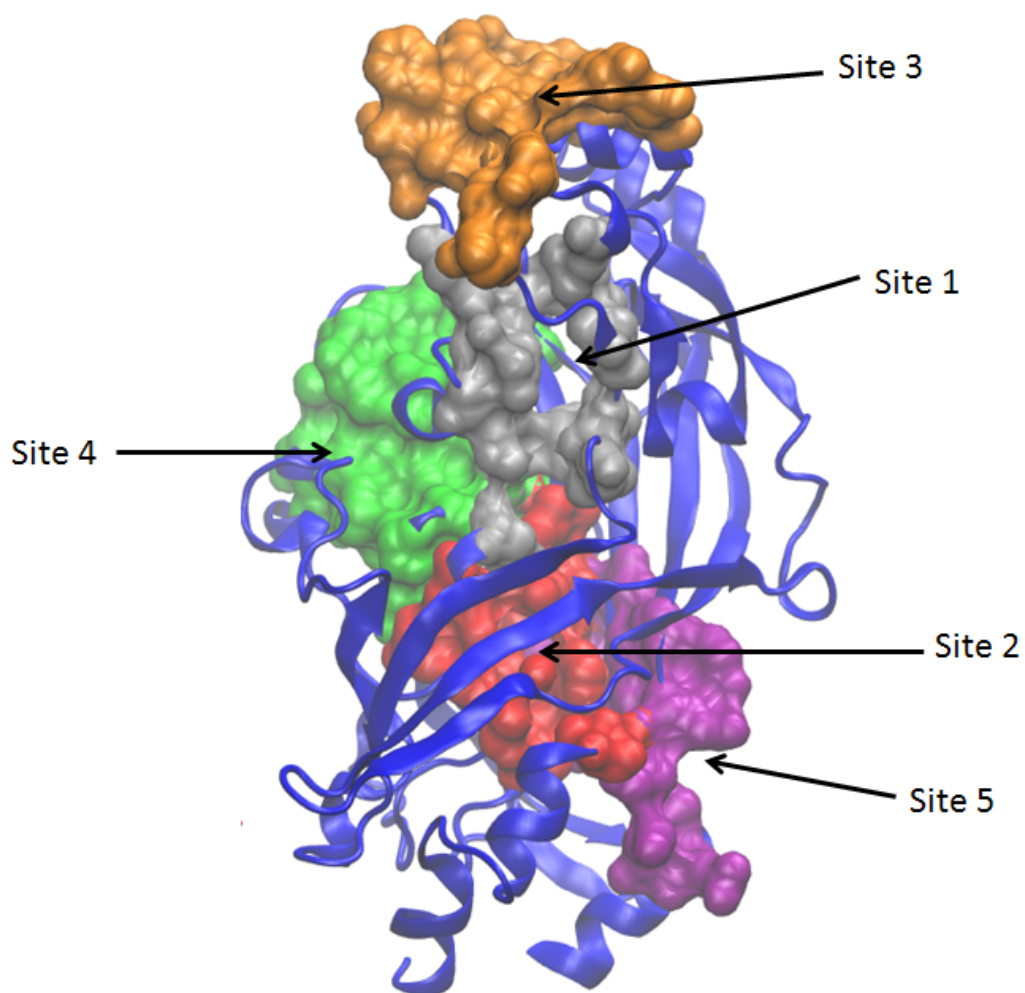


Figure S3: Graphic representation of the 3D structure of hCD36. The surface area of the binding pockets targeted for molecular docking are displayed: gray (site 1), red (site 2), orange (site 3), green (site 4), and purple (site 5).

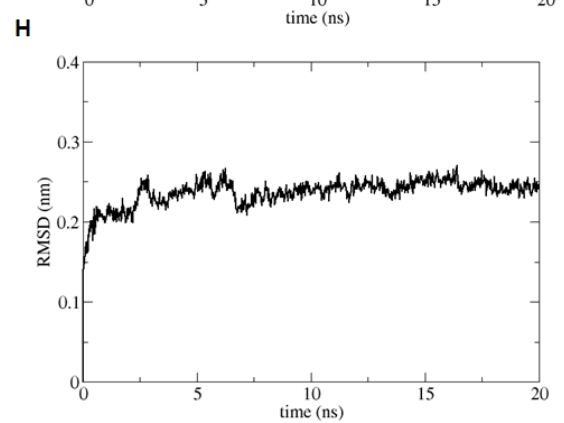
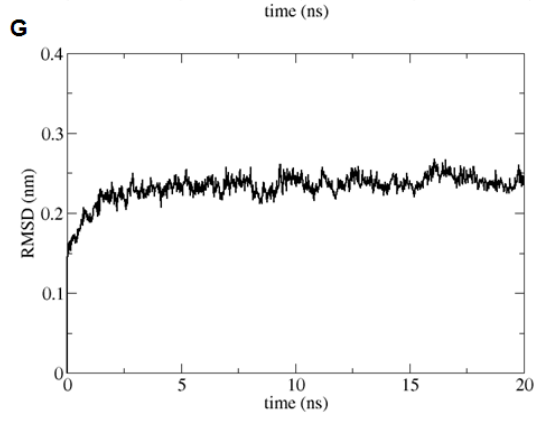
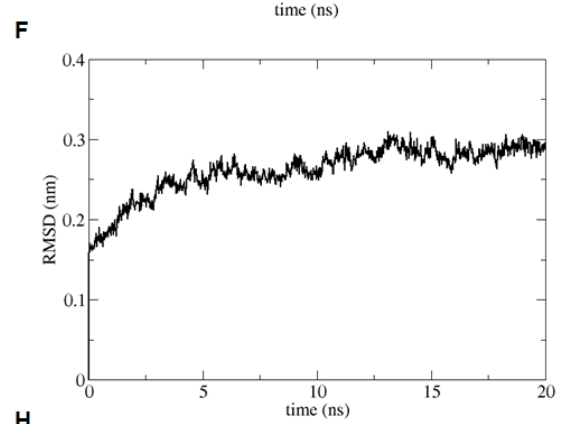
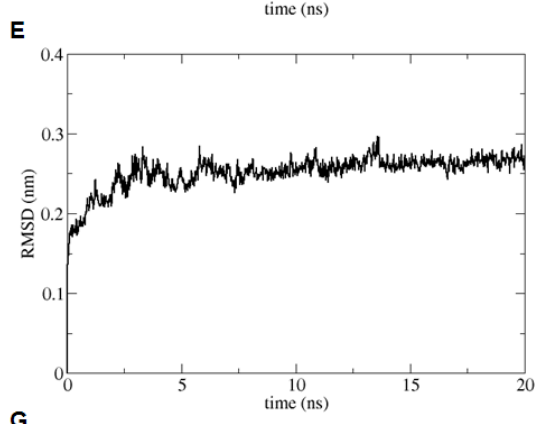
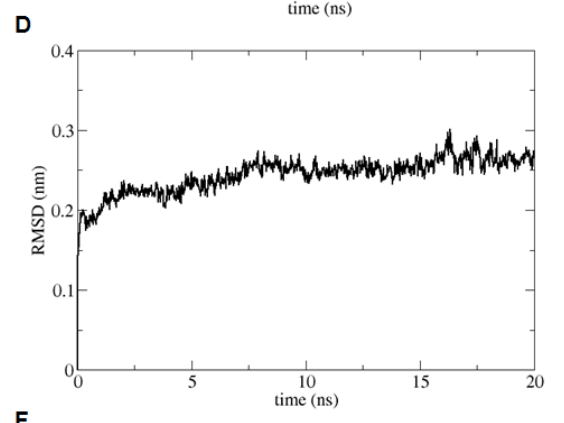
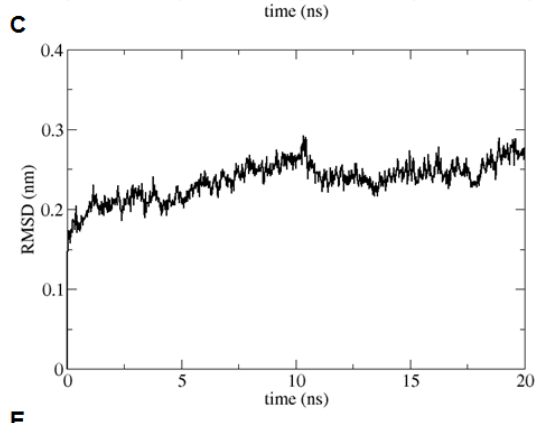
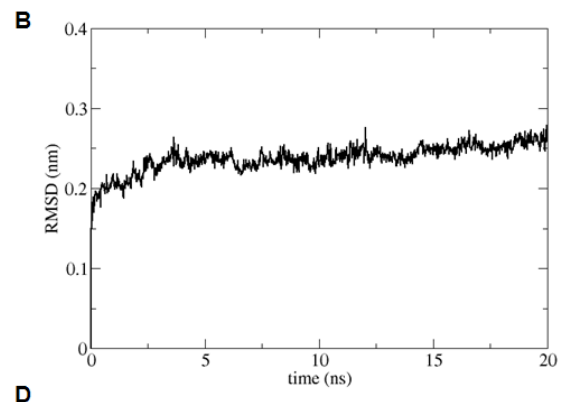
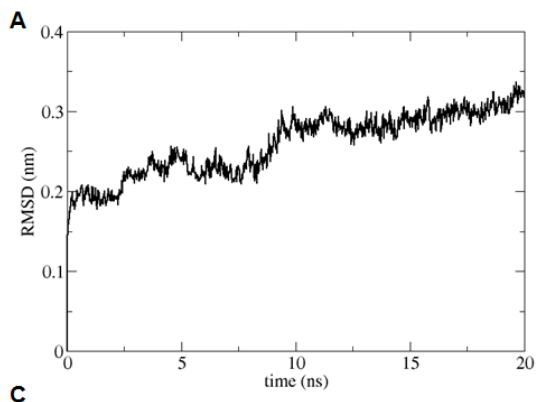


Figure S4: Time evolution of instantaneous RMSD values for heavy atom of the hCD36:Inhibitor complexes. A) Compound 3, B) Compound 4, C) Compound 5, D) Compound 6, E) Compound 7, F) Compound 8, G) Compound 9, H) Ursolic Acid (UA).

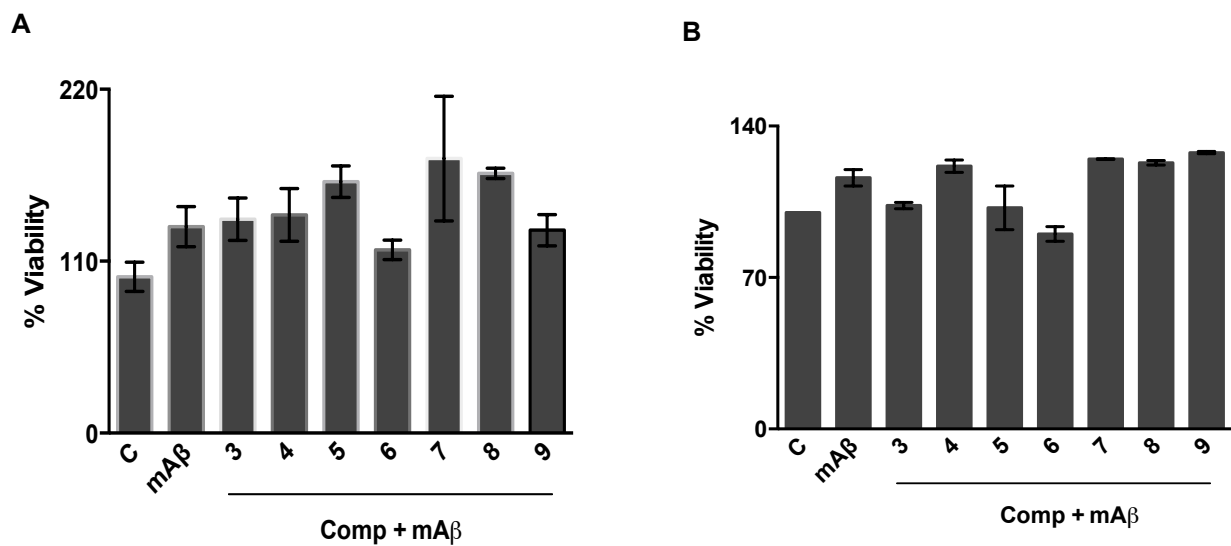


Figure S5: Compounds are not cytotoxic for peritoneal macrophages. Resazurin assay was used to determine the viability of the peritoneal macrophages from the experiments presented in figure 5. Resazurin method was performed in cells cultures after supernatant collection. (A) Viability of cells from the experiment represented in figures 5B and C. (B) Viability of cells from the experiment represented in figure 5D. Results represent means \pm S.E.M. from stimulus performed in duplicated and are representative of two independent experiments.

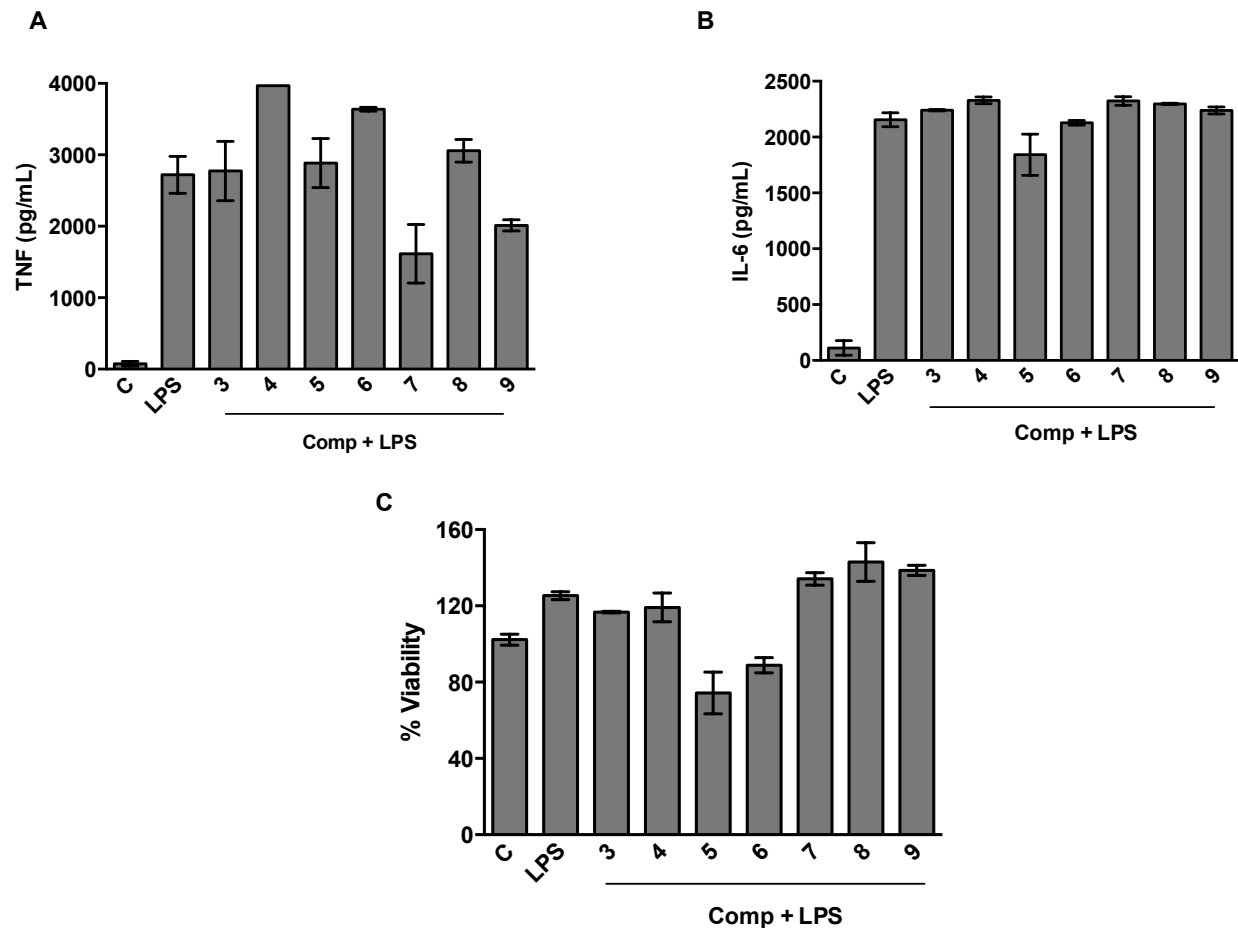
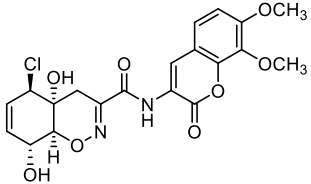
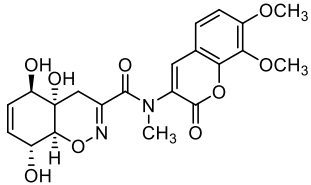
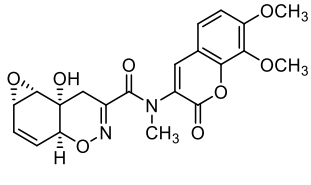
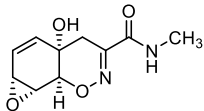
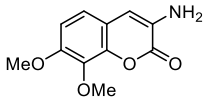
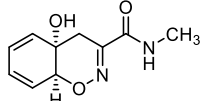
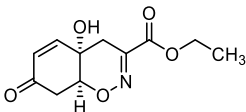
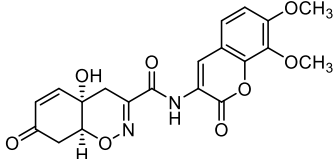
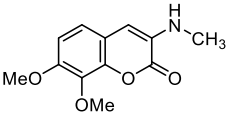
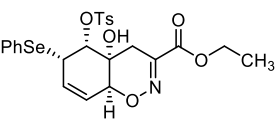
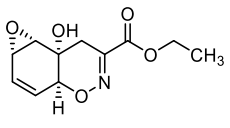
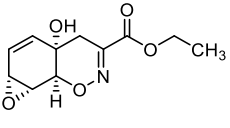
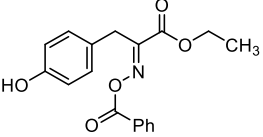
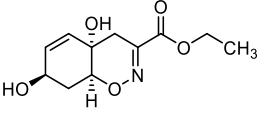
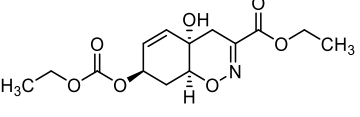
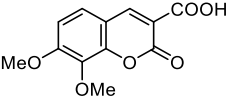
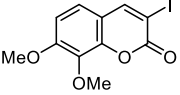


Figure S6: Trichoderamide analogues have no generalized effect on LPS response.

Macrophages from C57Bl/6 were stimulated with LPS (10 ng/ml) in the presence or absence of compounds (30 μ M). Supernatants were harvested 16 h after the stimulus and TNF- α (A) and IL-6 (B) levels were measured by the ELISA method. (C) Viability was assessed by the resazurin method after supernatant collection. Results represent means \pm S.E.M from stimulus performed in duplicated and are representative of three independent experiments.

Table S1. Effect of the Trichoderamide analogues on CD36-A β interaction.

Compound Code	2D Structure	IC ₅₀ (μ M)
2		NA
10		NA
11		NA
12		NA
13		NA
14		NA
15		NA
16		NA

17		NA
18		NA
19		NA
20		NA
21		NA
22		NA
23		NA
24		NA
25		NA

NA: non-active

Table S2. Residues in the binding sites of hCD36 target by molecular docking with Autodockvina.

Binding site^a	Residues
1	L140, A141, V142, A144, I148, L187, V198, L200, F201, D270, K334, R337, V339, I341, V389
2	T57, T59, V61, R63, R96, Q116, A251, A252, F266, F267, S268, I271, R273, I275, L295, F300, L328, I341, L343, T369, L371, T380, F383, K385, R386, L387, E418
3	N151, Q152, F153, V154, M156, I157, S160, K164, P191, Y192, P193, K398, Q400
4	I271, R273, I275, A299, F300, A301, S302, P303, N309, F312, C313, T314, E315, I318, S319, C322, S324, Y325, G326, V327, L328, D329, Y340, I341, S342, L343, V353, I410
5	G58, T59, E60, Y62, E365, R368, Y370, N382, R386, N417, G420, T421, G423, K426

a

^aCavities were identified using the Castp web server (<http://sts.bioengr-uic.edu/castp>)

Table S3. Binding free energies of the molecular docking of each ligand targeting different binding sites of the human CD36.

Compound code	ΔG^a (kcal/mol)				
	Site 1	Site 2	Site 3	Site 4	Site 5
3	-7.6	-7.9	-3.9	-6.3	-6.9
4	-8.1	-9.0	-3.5	-6.5	-5.8
5	-3.1	-6.3	18.8	6.1	2.2
6	-7.8	-8.5	8.1	-5.9	-6.2
7	-5.6	-6.5	-4.3	-5.6	-5.3
8	-5.8	-7.0	-4.4	-5.7	-5.1
9	-5.6	-6.5	-3.9	-6.1	-5.2
ursolic acid	-5.0	-6.0	-3.5	15.30	-5.0

^aCalculated using the Autodock Vina scoring function¹³.

Table S4. Summary of the electrostatic, van der Waals contributions, β , γ , D parameters used to calculated the binding free energy of the 8 CD36-ligand complexes

Compound Code	$\Delta\langle V_{l-s}^{el} \rangle$ (kcal/mol)	$\Delta\langle V_{l-s}^{vdw} \rangle$ (kcal/mol)	β^a	D ^b (kcal/mol)	γ^c (kcal/mol)	ΔG_{polar}^d (kcal/mol)	$\Delta G_{non-polar}^e$ (kcal/mol)
3	26.15	-23.64	0.37	13.93	-15.30	9.68	-19.55
4	19.11	-20.78	0.37	10.81	-12.33	7.07	-16.07
5	27.54	-27.30	0.37	15.10	-16.41	10.19	-21.32
6	6.04	-21.54	0.31	5.75	-7.52	1.87	-11.40
7	6.33	-12.83	0.37	4.65	-6.48	2.34	-8.79
8	14.25	-18.36	0.37	8.58	-10.21	5.27	-13.71
9	-7.89	-13.21	0.37	-0.54	-1.54	-2.92	-3.92
ursolic acid	6.67	-12.37	0.34	4.49	-6.33	2.27	-8.56

^aCalculated using parameterization model E of Almlöf *et al.*¹⁴

^b Calculated using the D parameter equation defined by Miranda *et al.*¹⁵
 $D = \beta\Delta\langle V_{l-s}^{el} \rangle - \alpha\Delta\langle V_{l-s}^{vdw} \rangle$ [kcal/mol]

^cCalculated using the γ parameter equation defined by Miranda *et al.*¹⁵ $\gamma = f * D + g$ [kcal/mol] where $f=-0.95$, and $g=-2.06$.

^d Polar component of the binding free energy $\Delta G_{polar} = \beta \times \Delta\langle V_{l-s}^{el} \rangle$.

^e Non-polar component of the binding free energy $\Delta G_{non-polar} = \alpha \times \Delta\langle V_{l-s}^{vdw} \rangle + \gamma$.

References

1. Mfuh, A. M.; Zhang, Y.; Stephens, D. E.; Vo, A. X.; Arman, H. D.; Larionov, O. V., Concise Total Synthesis of Trichodermamides A, B, and C Enabled by an Efficient Construction of the 1,2-Oxazadecaline Core. *J Am Chem Soc* 2015, *137* (25), 8050-3.
2. Berendsen, H. J. C., Postma, J. P. M., van Gunsteren, W. F., and Hermans, J, Interaction models for water in relation to protein hydration *In Intermolecular Forces (Pullman,B., ed.), Reidel, Dordrecht, The Netherlands* 1981, 331-342.
3. Hess, B.; Bekker, H.; Berendsen, H. J. C.; Fraaije, J. G. E. M., LINCS: A Linear Constraint Solver for Molecular Simulations. *J. Comput. Chem.* 1997, *18*, 1463-1476.
4. Miyamoto, S.; Kollman, P. A., Settle: An Analytical Version of the SHAKE and RATTLE Algorithm for Rigid Water Models. *J. Comput. Chem.* 1992, *13*, 952-962.
5. Verlet, L., Computer "Experiments" on Classical Fluids. I. Thermodynamical Properties of Lennard-Jones Molecules. *Phys. Rev.* 1967, *159*, 98-103.
6. Berendsen, H. J. C.; Postma, J. P. M.; van Gunsteren, W. F.; Dinola, A.; Haak, J. R., *J Chem Phys* 1984, *81*.
7. Berendsen, H. J. C.; Postma, J. P. M.; DiNola, A.; Haak, J. R., Molecular Dynamics with Coupling to an External Bath. *J. Chem. Phys.* 1984, *81*, 3684-3690.
8. van Gunsteren, W. F.; Berendsen, H. J. C., A Leap-Frog Algorithm for Stochastic Dynamics. *Mol. Simul.* 1988, *1*, 173-185.
9. Parrinello, M.; Rahman, A., Polymorphic Transitions in Single Crystals: A New Molecular Dynamics Method. *J. Appl. Phys.* 1981, *52*, 7182-7190.
10. Darden, T.; York, D.; Pedersen, L., Particle Mesh Ewald: An $W \log(N)$ Method for Ewald Sums in Large Systems. *J. Chem. Phys.* 1993, *98*, 10089-10093.
11. Essmann, U.; Perera, L.; Berkowitz, M. L.; Darden, T.; Lee, H.; Pedersen, L. G., A Smooth Particle Mesh Ewald Method. *J. Chem. Phys.* 1995, *103*, 8577-8592.
12. van der Spoel, D.; Lindahl, E.; Hess, B.; van Buuren, A. R.; Apol, E.; Meulenhoff, P. J.; Tieleman, D. P.; Sijbers, A. L. T. M.; Feenstra, K. A.; van Drunenand, R.; Berendsen, H. J. C., Gromacs User Manual version 4.5.6. Royal Institute of Technology and Uppsala University: Sweden, 2010.
13. Trott, O.; Olson, A. J., AutoDock Vina: Improving the speed and accuracy of docking with a new scoring function, efficient optimization, and multithreading. *J. Comput. Chem* 2010, *31* (2), 455-461.
14. Almlof, M.; Carlsson, J.; Aqvist, J., Improving the Accuracy of the Linear Interaction Energy Method for Solvation Free Energies. *J. Chem. Theory Comput.* 2007, *3*, 2162-2175.
15. Miranda, W. E.; Noskov, S. Y.; Valiente, P. A., Improving the LIE Method for Binding Free Energy Calculations of Protein–Ligand Complexes. *Journal of Chemical Information and Modeling* 2015, *55* (9), 1867-1877.